PNAS RESEARCH ARTICLE | GENETICS

Orc6 is a component of the replication fork and enables efficient mismatch repair

Yo-Chuen Lin[a], Dazhen Liu[a], Arindam Chakraborty[a], Lyudmila Y. Kadyrova[b], You Jin Song[a], Qinyu Hao[a], Jaba Mitra[c], Rosaline Y. C. Hsu[a], Mariam K. Arif[a], Sneha Adusumilli[a], Ting-Wei Liao[c], Taekjip Ha[c,d], Farid A. Kadyrov[b], Kannanganattu V. Prasanth[a,e], and Supriya G. Prasanth[a,e,1]

Edited by Jasper Rine, University of California, Berkeley, CA; received November 24, 2021; accepted March 24, 2022

In eukaryotes, the origin recognition complex (ORC) is required for the initiation of DNA replication. The smallest subunit of ORC, Orc6, is essential for prereplication complex (pre-RC) assembly and cell viability in yeast and for cytokinesis in metazoans. However, unlike other ORC components, the role of human Orc6 in replication remains to be resolved. Here, we identify an unexpected role for hOrc6, which is to promote S-phase progression after pre-RC assembly and DNA damage response. Orc6 localizes at the replication fork and is an accessory factor of the mismatch repair (MMR) complex. In response to oxidative damage during S phase, often repaired by MMR, Orc6 facilitates MMR complex assembly and activity, without which the checkpoint signaling is abrogated. Mechanistically, Orc6 directly binds to MutSα and enhances the chromatin-association of MutLα, thus enabling efficient MMR. Based on this, we conclude that hOrc6 plays a fundamental role in genome surveillance during S phase.

ATR | DNA damage | mismatch repair | Orc6 | replication

Significance

Origin recognition complex (ORC) is required for the initiation of DNA replication. Unlike other ORC components, the role of human Orc6 in replication remains to be resolved. We identified an unexpected role for hOrc6, which is to promote S-phase progression after prereplication complex assembly and DNA damage response. Orc6 localizes at the replication fork, is an accessory factor of the mismatch repair complex, and plays a fundamental role in genome surveillance during S phase.

Accurate duplication of genetic material and faithful transmission of genomic information are critical to maintain genome stability. Errors in DNA replication and repair mechanisms are deleterious and cause genetic aberrations leading to malignant cellular transformation and tumorigenesis. Origin recognition complex (ORC) proteins are critical for the initiation of DNA replication (1), and the individual subunits of ORC also play vital roles in several non–prereplication complex (pre-RC) functions, including heterochromatin organization, telomere maintenance, centrosome duplication, and cytokinesis (2, 3). Mutations within several *ORC* genes, including *ORC1, ORC4, and ORC6*, have also been linked to Meier-Gorlin syndrome, a rare genetic disorder in children, characterized by primordial dwarfism (4–6).

ORC serves as the landing pad for the assembly of the multiprotein pre-RC at the origins of replication during G1 (7). The smallest subunit of ORC, Orc6, is highly dynamic with respect to its association with the other ORC components (8–10). Orc6 is an integral part of ORC in yeast and *Drosophila* (1, 11), but only weakly associates with ORC in human and *Xenopus* (8, 10, 12, 13). Orc6 possesses DNA binding ability and is believed to be critical for DNA replication initiation in all eukaryotes (14–18); however, human Orc6 and Orc1-5 can bind to DNA independently (19). There is evidence that hOrc6 protein directly binds to the Orc3 subunit and integrates as a part of ORC in vivo in human cell lines (9). However, a substantial fraction of hOrc6 is not associated with the ORC, and depletion of other ORCs does not alter hOrc6 chromatin association, suggesting that hOrc6 is involved in ORC-independent functions within the cell (10, 13, 20). In support of this, metazoan Orc6 is also required for cytokinesis (17, 21, 22). In yeast, Orc6 is dispensable for progression through mitosis and cytokinesis, but the depletion of Orc6 after pre-RC assembly has been shown to impair replication origin firing (15). However, to our knowledge, no such role for Orc6 has been evaluated in higher eukaryotes.

Accurate duplication of the genetic material and correction of errors during S phase are efficiently coordinated with the machinery that ensures genomic integrity (23). Mismatches occurring during DNA replication are recognized and removed by the mismatch repair (MMR) system. The key components of the MMR system that have been identified to date are MutSα (MSH2-MSH6 complex), MutSβ (MSH2-MSH3 complex), MutLα (MLH1-PMS2 complex), RFC-loaded PCNA, and exonuclease 1 (EXO1) (24). The association of MMR machinery to the replication fork is facilitated by PCNA, an essential replication factor that is also required for MMR (25–29). In eukaryotes, MMR is active throughout the cell cycle, with the highest activity observed during S phase (30–32). Several replication accessory factors, chromatin-associated factors, and epigenetic regulators also influence MMR (33–38), yet the functional relevance of these interactions has not been well understood.

Author contributions: Y.C.L., D.L., A.C., and S.G.P. designed research; Y.C.L., D.L., A.C., L.Y.K., J.M., R.Y.C.H., M.K.A., S.A., T.W.L., and S.G.P. performed research; Y.C.L., L.Y.K., Y.J.S., Q.H., M.K.A., S.A., F.A.K., and K.V.P. contributed new reagents/analytic tools; Y.C.L., D.L., A.C., J.M., T.H., F.A.K., K.V.P., and S.G.P. analyzed data; and Y.C.L. and S.G.P. wrote the paper.

The authors declare no competing interest.

This article is a PNAS Direct Submission.

[1]To whom correspondence may be addressed. Email: supriyap@illinois.edu.

This article contains supporting information online at http://www.pnas.org/lookup/suppl/doi:10.1073/pnas.2121406119/-/DCSupplemental.

Published May 27, 2022.

We report that hOrc6 associates with the replication fork and is primarily required for DNA replication progression but not for G1 licensing. During S phase, Orc6 forms an integral component of the MMR complex and controls MMR complex assembly and activity. Loss of Orc6 results in defective MMR activity, resulting in loss of ATR signaling. Based on our results, we conclude that hOrc6 has a fundamental role in genome surveillance during S phase.

RESULTS

Orc6 Is a Component of the Replication Fork. Using isolation of proteins on nascent DNA (iPOND), we found that hOrc6 associates with the replication fork in vivo. Nascent DNA was labeled with EdU, conjugated with biotin, and proteins associated with biotin-EdU–labeled DNA were pulled down. Thymidine chase was also performed to allow EdU labeling to move past nascent DNA, away from the replication fork and into mature DNA. Therefore, thymidine chase was used to label the mature chromatin as a control. Orc6 accumulated on nascent DNA, whereas it did not enrich on the mature DNA (Fig. 1*A*). Orc2, a component of the core ORC, was found both on nascent and mature chromatin, consistent with it being a chromatin-associated factor. To confirm the association of Orc6 with the replication fork and gain quantifiable results, we performed quantitative in situ analysis of protein interactions at DNA replication forks (SIRF) (39). Nascent DNA was labeled with EdU, conjugated with biotin, and then proximity ligation assay (PLA) was performed to determine the association between hOrc6 and biotin-EdU–labeled DNA. Thymidine chase was also done to distinguish the association of hOrc6 with nascent versus mature DNA. SIRF experiments also showed that hOrc6 associated with nascent DNA (Fig. 1*B*). Similar to our observation, hOrc6 was found in proteomic screens of proteins enriched in nascent DNA by nascent chromatin capture (stable isotope labeling of amino acids in cell culture $\log_2$ ratio = 0.76 ± 0.45) (40) as well as by iPOND ($\log_2$ ratio = 1.28) (41), suggesting its association with replication forks in human cells. Furthermore, immunoprecipitation experiments (Fig. 1*C*) and single-molecule pull down assays (*SI Appendix*, Fig. S1 *A* and *B*) demonstrated that hOrc6 interacted with several replication-fork components, including the single-stranded DNA (ssDNA) binding protein RPA, the DNA clamp PCNA, and the clamp loader RFC. These results demonstrate that hOrc6 is enriched at the replication fork and associates with the fork components, implying that Orc6 in human cells could be involved in functions downstream of pre-RC assembly.

Orc6 Is Required for Accurate S Phase Progression. In *Saccharomyces cerevisiae*, when Orc6 was depleted during late G1, MCM proteins were displaced from chromatin, and cells failed to progress through S phase, suggesting that efficiency of replication origin firing was compromised (15). However, a similar role has not been evaluated for Orc6 in higher eukaryotes, to our knowledge. The depletion of Orc6 in human cells with an intact p53-mediated checkpoint status caused a decrease in S-phase population with a concomitant reduction in the chromatin association of PCNA (Fig. 1*D* and *SI Appendix*, Fig. S1*C*); however, this could be either due to a role in S phase or to the role of Orc6 during G1. Since we observed the association of hOrc6 with nascent DNA (Fig. 1 *A* and *B*), we assessed the role of hOrc6 in post-G1 cells. We utilized a degron system, which allows degradation of Orc6 by ubiquitin-proteasomal degradation at any specific time point during the cell cycle (42). We tagged hOrc6 with a destruction domain (DD); the DD tag is recognized by the proteasomal machinery and facilitates the rapid degradation of the DD-Orc6. In the presence of Shield1, a molecule that masks the DD tag, DD-Orc6 is prevented from degradation (Fig. 1*E*). DD-Orc6 could substitute for endogenous Orc6, as the tagged-hOrc6 rescued the cell-cycle defects observed in cells depleted of endogenous hOrc6 (compare samples 2 and 3 in *SI Appendix*, Fig. S1 *D* and *E*). We depleted the endogenous Orc6 using small interfering RNA targeting the 3′–untranslated region of Orc6 in U2OS cells stably expressing DD-Orc6 and carried out the experiment in the presence of Shield1. We then synchronized the cells at the G1/S boundary, degraded DD-Orc6 by removing Shield1, and evaluated the effect of hOrc6 loss in post-G1 cells on progression through S phase (Fig. 1*F*). The degradation of hOrc6 in post-G1 cells resulted in defects of progression through S phase. The propidium iodide (PI) flow profile at the 4- to 8-h time point after thymidine release revealed that more cells progressed through S phase in control cells than in Orc6-depleted cells (Orc6-si1 and -si2 lack endogenous as well as DD-Orc6; Fig. 1*G*). The BrdU-PI profile further corroborated these results demonstrating the defects in S-phase progression of thymidine-released post-G1 cells in the absence of hOrc6 (Fig. 1*H*).

Since Orc6 is part of the ORC and studies from yeast and *Drosophila* all point to its involvement in origin licensing (6, 43), we also utilized our degron system to examine the presumed function of hOrc6 in G1 licensing. We synchronized the DD-Orc6–expressing cells depleted of endogenous Orc6 into early G1 phase (*SI Appendix*, Fig. S1*F*) and degraded DD-Orc6 by removing Shield1. By determining the loading of pre-RC components onto chromatin in G1 cells lacking Orc6, we monitored the chromatin association of pre-RC components (Orc2, Cdt1, MCM3). Surprisingly, the chromatin loading of these factors remained unaffected in the cells depleted of hOrc6, suggesting that Orc6 might be dispensable for replication licensing in human cells or the small levels of Orc6 left in cells were sufficient to load MCMs (*SI Appendix*, Fig. S1*G*).

To confirm this further, we used flow cytometry to measure MCM licensing status, in conjugation with cell-cycle analysis (44). Cells were extracted using detergent before fixing to remove soluble MCMs. The chromatin-bound MCMs served as an indicator of origin licensing and were detected by immunostaining with MCM3 antibody (*SI Appendix*, Fig. S1*H*). Strikingly, hOrc6-depleted cells had a similar amount of chromatin-bound MCMs in the G1 population to control cells, again suggesting that the depletion of Orc6 did not alter the MCM association to the chromatin (*SI Appendix*, Fig. S1 *I* and *J*). In contrast, Orc1 knockdown showed a severe licensing defect, as indicated by a dramatic reduction of chromatin-bound MCMs (*SI Appendix*, Fig. S1 *I* and *J*). However, even with proper licensing, hOrc6-depleted cells were unable to efficiently progress through S phase, indicating a critical role of hOrc6 in S-phase progression.

Loss of Orc6 Sensitizes Cells to DNA Damage, and Orc6-Depleted Cells Fail to Activate ATR in Response to Replicative Stress. Cells with replication defects often show reduced tolerance toward replication stress and DNA damage. Because we observed defects in progression of cells through S phase upon Orc6 depletion (Fig. 1 *G* and *H*), we examined the replication fork dynamics in hOrc6-depleted cells upon replication-stress treatment. Cells were first labeled with CldU for 30 min, treated with hydroxyurea (HU) for 2 h to induce stalling of the

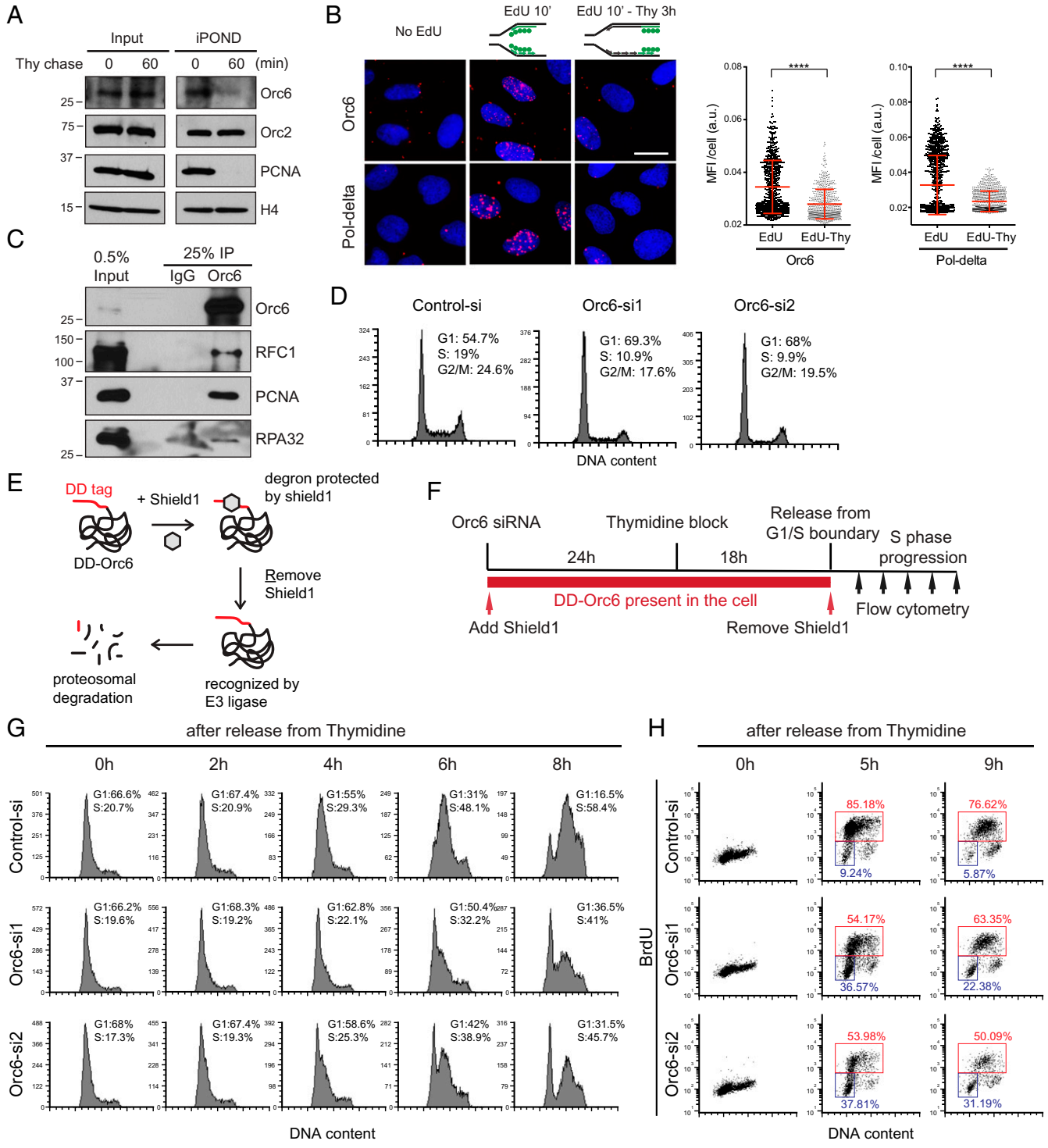

Fig. 1. Orc6 is at nascent DNA and required for proper S-phase progression. (*A*) Western blot of iPOND. Thymidine chase (0 min) for nascent DNA and 60 min for mature DNA. PCNA as a positive control for nascent DNA. (*B*) Representative images for SIRF in U2OS cells (*Upper*). Red foci indicate the association between Orc6 and EdU-biotin. PLA of Pol-δ/Edu-biotin served as a positive control; DAPI was a counterstain. Scale bar, 25 μm. (*Lower*) Quantification results. Experiments were performed in triplicate and one representative experiment is shown; $n > 700$ for each group. Data are reported as mean ± SD. ****$P < 0.0001$ by Mann-Whitney test. (*C*) Immunoprecipitation of endogenous Orc6 from U2OS cells. (*D*) Cell cycle profile of Orc6 knockdown in U2OS cells. (*E*) Schematic illustration of the DD degron system for controlling the degradation of DD-Orc6. (*F*) Schematic of the protocol for specifically depleting Orc6 in S phase. (*G*) S phase progression determined by PI flow cytometry. (*H*) S-phase progression determined by BrdU-PI flow cytometry. a.u., arbitrary unit; IP, immunoprecipitation; MFI, mean fluorescence intensity; Thy, thymidine.

replication fork, and were subsequently released into fresh medium containing IdU for another 30 min. DNA combing assay revealed that the cells lacking hOrc6 had a significant and consistent decrease in fork restart (Fig. 2*A*). This result implies that the S-phase progression defects observed in hOrc6-depleted cells could be attributed to defects in the fork restart.

To test if the defective progression through S phase resulted in replication stress and/or DNA damage, we performed a comet assay to assess the extent of DNA breaks in hOrc6-depleted cells. There were no obvious double- or single-strand breaks observed with the comet assay in the absence of hOrc6 under unperturbed conditions. However, hOrc6-depleted cells in the presence of

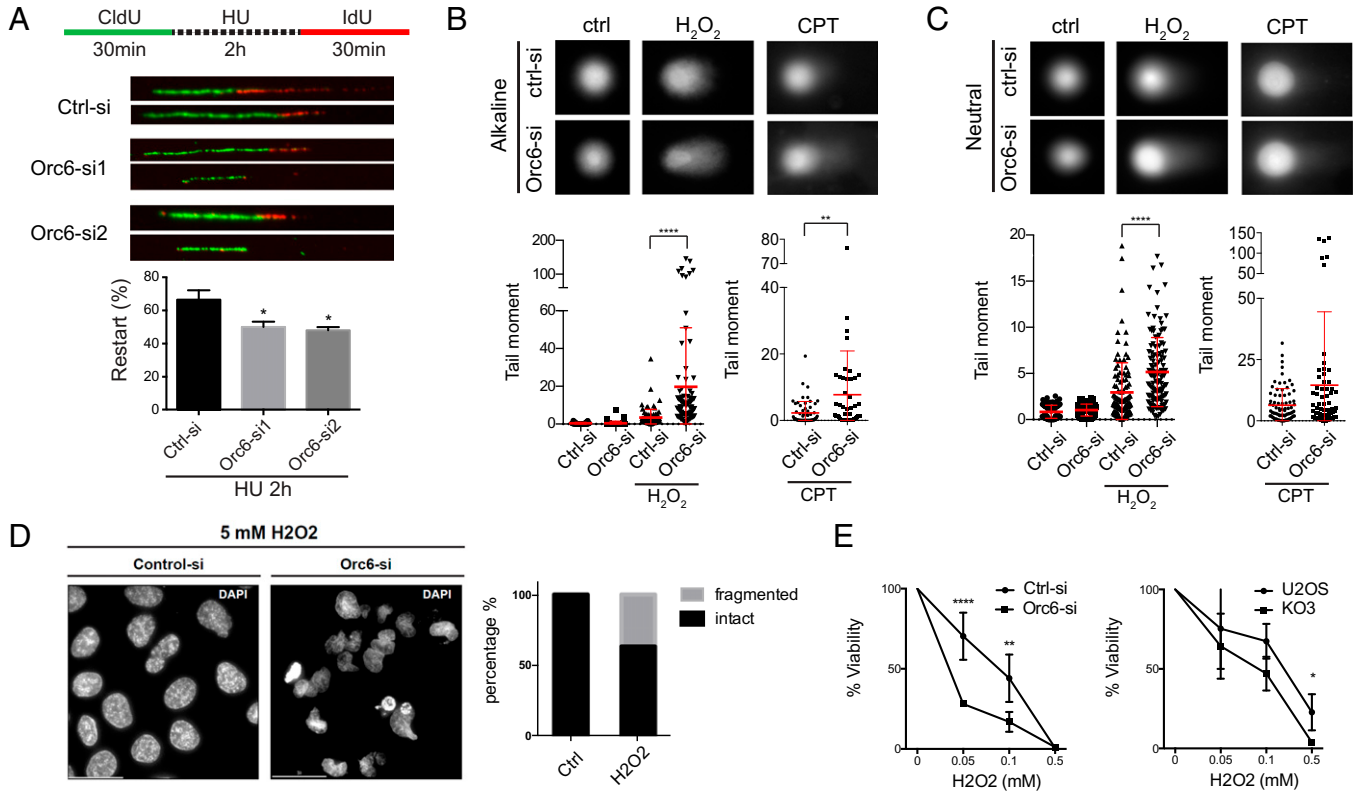

Fig. 2. Depletion of Orc6 sensitizes cells to DNA damage. (*A*) Representative images of DNA fiber (*Upper*). Control (ctrl) or knockdown U2OS cells were labeled with HU 2 mM for 2 h between CldU and IdU labeling. (*Lower*) Percentages of restart tracks in total tracks counted. Data reported as mean ± SD; $n = 3$. *$P < 0.05$ by unpaired two-tailed Student *t* test. (*B*) Alkaline comet assay. Cells were treated with control, H_2O_2 (0.5 mM for 3 h) or camptothecin (CPT; 10 μM for 4 h) before collecting for comet assay. (*Upper*) Representative images are shown. One representative experiment for each is shown for H_2O_2-treated ($n = 5$) and CPT-treated ($n = 2$) cells. Data are reported as mean ± SD. **$P < 0.01$, ****$P < 0.0001$ by Mann-Whitney test. (*C*) Neutral comet assay. Cells were treated the same as in the alkaline comet assay. (*Upper*) Representative images are shown. Data are reported as mean ± SD. *$P < 0.05$, ****$P < 0.0001$ by unpaired two-tailed Student *t* test. (*D*) DAPI staining of control or Orc6 knockdown cells treated with H_2O_2. Scale bar, 30 μm. Percentages of intact and fragmented nuclei are shown in the bar chart (*Right*). (*E*) Clonogenic survival assay of H_2O_2-treated control and Orc6 knockdown cells (*Left*); control and Orc6 knockout cells (*Right*). Data are reported as mean ± SD; $n = 3$. *$P < 0.05$, **$P < 0.01$, ****$P < 0.0001$ by unpaired two-tailed Student *t* test.

DNA damaging agents, including camptothecin and hydrogen peroxide (H_2O_2) had increased levels of DNA damage compared with wild-type (WT) cells, as observed by both alkaline and neutral comet assays (Fig. 2 *B* and *C*). Furthermore, hOrc6-depleted or hOrc6-knockout cells were sensitive to DNA damage, as observed by significant nuclear fragmentation and decreased cell survival after H_2O_2 treatment (Fig. 2 *D* and *E*). We reasoned that in the absence of hOrc6, the cells either fail to repair the damage or fail to sense DNA damage.

We treated U2OS cells (with or without Orc6) with various DNA damaging agents, including H_2O_2 (oxidative damage), neocarzinostatin (a radiomimetic drug), and HU for 4 h (to induce ssDNA and replication stress due to fork stalling) or for 24 h (to induce fork collapse and double-strand breaks [DSBs]), and monitored the activation of ATR and ATM. The cells lacking Orc6 failed to activate ATR, as evident by decreased phospho-Chk1 and phospho-RPA levels, in response to different DNA damaging agents (Fig. 3 *A* and *B* and *SI Appendix*, Fig. S2*A*). However, the ATM remained active, as evident by intact Chk2 phosphorylation in both control and hOrc6-depleted cells. On the other hand, ATR activation was not impaired as dramatically by the depletion of the other ORC subunits (Orc1 and Orc2) (note * hyperphosphorylation of RPA32 in Fig. 3*B*). DNA-damaged cells lacking hOrc6 also showed reduced chromatin association of RPA, as observed by immunofluorescence staining using RPA antibodies following pre-extraction procedures (Fig. 3*C*).

We next examined if the defects in RPA phosphorylation and Chk1 phosphorylation in cells lacking hOrc6 are a result of defective replication or if they are due to a direct role of hOrc6 in the ATR pathway. We synchronized the DD-Orc6–expressing cells (control cells as well as endogenous Orc6-depleted cells) in S phase by thymidine block, and we subsequently degraded DD-Orc6 by removing Shield1 from the medium after the cells were released into S phase. We then induced DNA damage in the control and hOrc6-depleted, S phase–synchronized cells (Fig. 3*D*) and determined the status of ATR activity. We continued to observe defective ATR activation, as evident by reduced pChk1 and pRPA in Orc6-depleted cells that had been accumulated in S phase (Fig. 3*D*). In addition, we synchronized control and hOrc6 knockout cells (hypomorph) into G2 phase and treated them with DNA damaging agents. The control G2 cells showed robust Chk1 phosphorylation, whereas the Orc6-KO G2 cells failed to activate ATR, suggesting that hOrc6 facilitates ATR activation and that ATR activation defects in Orc6-depleted cells are not because of cell-cycle effects (Fig. 3*E*). These results support our model that hOrc6 is required for ATR activation and that the defects observed in Orc6-depleted cells are not simply a reflection of cell-cycle defects.

The defect in RPA32 phosphorylation in hOrc6-depleted cells indicates that Orc6 may be involved in the upstream steps of the ATR signaling pathway. Processing of different DNA damages by various repair pathways yields ssDNA as a critical repair intermediate, which also serves to activate ATR. The two

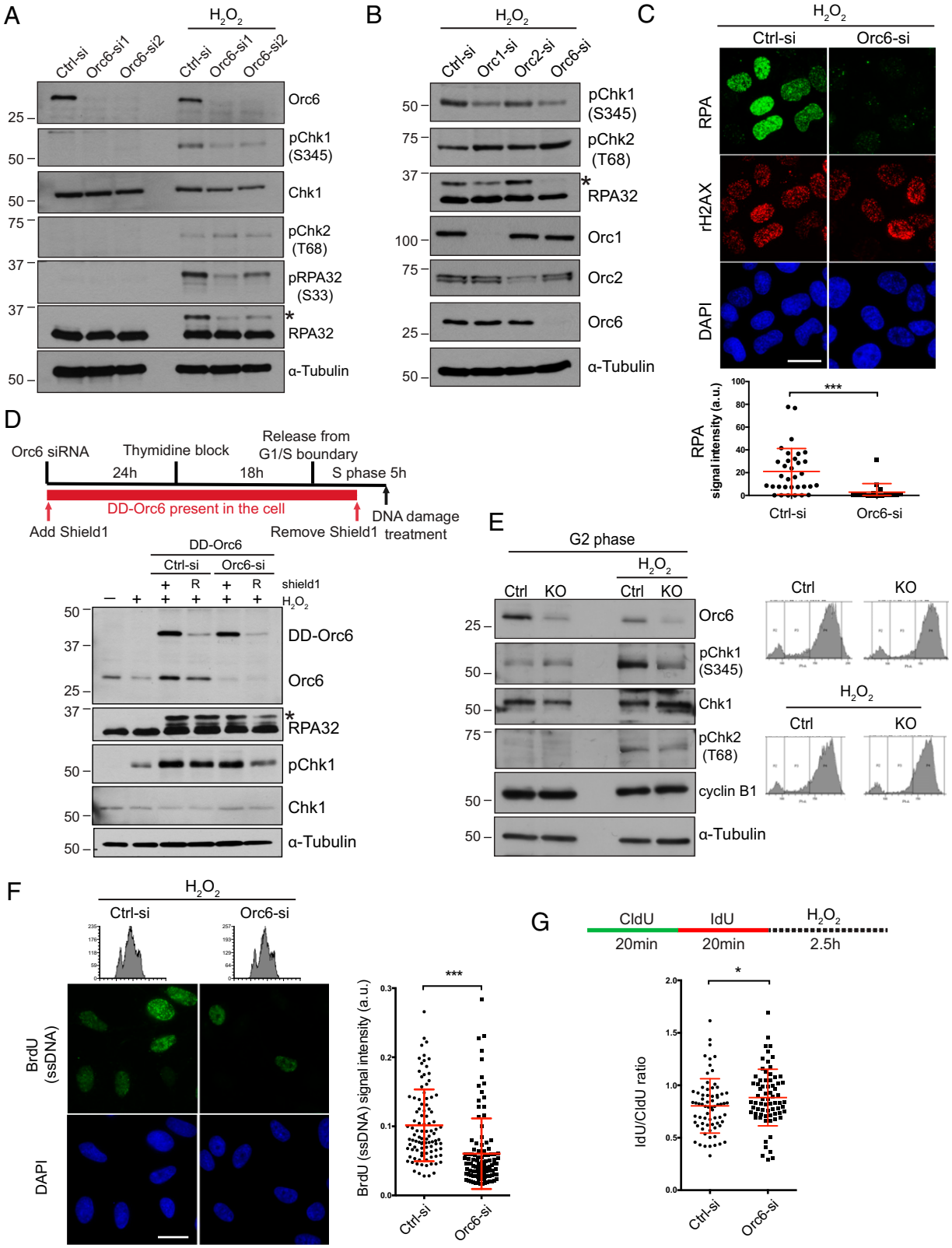

Fig. 3. Loss of Orc6 leads to compromised ATR signaling pathway due to reduced ssDNA generation. (*A*) Western blot analysis of the ATM/ATR pathway in control (Ctrl) and Orc6 knockdown U2OS cells. Hyperphosphorylation of RPA32 is indicated by the asterisk. (*B*) Western blot for Orc1, Orc2, and Orc6 knockdown cells. (*C*) Immunostaining of chromatin-associated RPA and rH2AX in control and Orc6-depleted cells treated with H_2O_2. Scale bar, 25 μm. Quantification of RPA signal is shown at bottom. Data are reported as mean ± SD. ***$P < 0.001$ by Mann-Whitney test. (*D*) Schematic of the protocol for specifically depleting Orc6 in S phase and collecting DNA damage samples (*Upper*). Shield1 was removed 1 h before H_2O_2 treatment and cells were collected 1 h after treatment. (*Lower*) Western blot for analyzing ATR activation. (*E*) Western blot of G2 synchronized control and Orc6 knockout (KO) cells. Cyclin B1 as G2 marker. PI flow profiles show the synchrony of the cells. (*F*) Native BrdU staining for visualizing ssDNA (*Right*) and quantification results (*Left*). Scale bar, 25 μm. PI flow profiles show the synchrony of the cells. A representative experiment ($n = 3$) is shown. Data are reported as mean ± SD; $n > 100$ for each group. ***$P < 0.001$ by Mann-Whitney test. (*G*) DNA fiber assay to determine nascent DNA resection or degradation after fork stalling. A higher IdU to CldU ratio indicates less resection, hence less ssDNA generation. A representative experiment ($n = 2$) is shown. Data are reported as mean ± SD. ****$P < 0.0001$ by unpaired one-tailed Student *t* test. a.u., arbitrary unit; R, removal of Shield1.

following possibilities could attribute to defects in ATR signaling upon hOrc6 depletion. First, hOrc6 could function in the recruitment of ATR signaling proteins to the RPA–ssDNA platform. Second, hOrc6 could play a role in generating ssDNA after DNA damage. To test if hOrc6 plays a direct role in ATR activation, we performed an in vitro assay to examine the recruitment of ATR signaling proteins onto the RPA–ssDNA platform in the presence or absence of hOrc6. We preassembled RPA–ssDNA complex by mixing recombinant RPA with 3′-biotinylated 70-mer ssDNA. We captured the complex using streptavidin-coated magnetic beads. These RPA–ssDNA structures were then incubated with nuclear extracts from control and Orc6-depleted U2OS cells, and we retrieved the proteins that bound to the structure. Western blotting was used to determine the effect of ATR signaling protein recruitment and activation, including RPA, ATR-interacting protein (ATRIP) that associates with ATR and mediates its interaction with RPA, and Chk1 (*SI Appendix*, Fig. S2*B*). We did not observe any defect in the recruitment of all of the proteins in the Orc6-depleted extract. We also determined if hOrc6 plays any role in the RPA association with ssDNA. We performed ssDNA in vitro pull down with hOrc6 first being added to ssDNA and then RPA, or vice versa (*SI Appendix*, Fig. S2*C*). Again, these experiments demonstrated that hOrc6 did not have a direct role in facilitating RPA association with ssDNA. Based on these experiments, we concluded that hOrc6 does not play any direct role in the recruitment of signaling proteins to ssDNA and subsequent ATR activation.

Next, we evaluated whether hOrc6-depleted cells compromised the levels of ssDNA in cells. We quantified the levels of ssDNA in control and hOrc6-depleted cells using BrdU staining under nondenaturing conditions. The DD-Orc6 cell line was used to ensure that both control and Orc6 knockdown cells were synchronized in S phase and had incorporated an equal amount of BrdU. We observed a significant reduction in ssDNA in cells lacking Orc6 (Fig. 3*F*). Based on these results, we conclude that hOrc6 supports the generation of ssDNA after DNA damage.

Our results suggest that the inability to generate ssDNA in hOrc6-depleted cells contributes to the defects in ATR activation. Many repair pathways require the generation of ssDNA, such as end resection after DSBs to allow homologous recombination. During excision repair and MMR pathways, ssDNA is also generated in a regulated manner by the removal of damaged bases and strands (45). Since we observed hOrc6 at the replication fork, we set out to determine the efficiency of ssDNA generation at the fork in cells lacking Orc6 under DNA-damage conditions. Cells labeled sequentially with CldU and IdU (20 min each) were immediately treated with a DNA damaging agent. The resection or degradation of a nascent DNA strand after DNA damage was then calculated by measuring the length of the IdU-labeled fiber in a DNA fiber assay. We observed that DNA-damaged cells lacking hOrc6 had a higher IdU to CldU ratio after 40 min, indicating defects in nascent DNA degradation (Fig. 3*G* and *SI Appendix*, Fig. S2*D*). This result further confirms that the reduced ability to generate ssDNA in hOrc6-depleted cells causes defects in ATR activation. However, given the modest level of ssDNA reduction we observed, there might be other mechanisms and other factors contributing to the defect in ATR signaling, and more investigation is needed.

Orc6 Associates with the MMR Complex by Interacting with MutSα and Supports MMR Phenotypes. To gain mechanistic insights into the role of hOrc6 in S-phase progression and in DNA damage response, we identified hOrc6-interacting proteins during S phase (in the presence or absence of DNA damage) by performing immunoprecipitation followed by mass spectrometry. The hOrc6-interacting proteome revealed known interactors as well as other previously unreported interactions (Dataset S1). Strikingly, we found that in S-phase extract, hOrc6 interacted with all the components of the MutSα (MSH2 and MSH6) and MutLα (MLH1 and PMS2) complexes that are known to initiate DNA MMR (Fig. 4*A*). More importantly, H_2O_2-treated cells revealed enhanced interaction between hOrc6 and members of the MMR complex, as well as increased RFC subunits. Being an essential factor for PCNA loading, RFC is also an important component of the MMR pathway (Fig. 4*A*). By analyzing the Orc6-interacting proteins using gene ontology enrichment and the Kyoto Encyclopedia of Genes and Genomes pathway, we also observed the DNA MMR pathway to be the highest-enriched category (*SI Appendix*, Fig. S3 *A* and *B*). We validated the in vivo association between hOrc6 and MSH2 using PLA. The interaction between hOrc6 and MSH2 was enhanced in oxidative stress–induced cells (Fig. 4*B*). Furthermore, the association between these two proteins became more significant in S-phase cells (Fig. 4*B*). To further examine the physical interaction of Orc6 with MutSα and MutLα, we conducted GST pull-down using purified proteins. We found that Orc6 directly interacts with MutSα but not MutLα (Fig. 4*C*). Moreover, GST pull down using Orc6 truncations identified that Orc6 interacts with MutSα through its middle TFIIB (TFIIB-B) domain (Fig. 4 *D* and *E*). To evaluate if Orc6 functions in the MMR pathway, we conducted a survival assay with cisplatin, since it is well established that MMR-deficient cells are tolerant to cisplatin treatment (46, 47). Orc6-depleted cells showed resistance toward cisplatin to a level similar to that of MSH6 knockdown (Fig. 4*F* and *SI Appendix*, Fig. S3*C*). Importantly, the double knockdown of Orc6 and MSH6 did not further increase the resistance, suggesting that they function in the same pathway. Moreover, Orc6 depletion also resulted in increased mutation frequency determined by HPRT assay (Fig. 4*G*), and the double depletion of Orc6 and MSH6 did not further increase the mutation frequency (*SI Appendix*, Fig. S3 *D* and *E*). Our results indicate that hOrc6 physically interacts with MutSα complex during S phase and during oxidative DNA damage, and supports the MMR.

Orc6 Promotes MutLα Recruitment to MutSα and Facilitates MMR Activity. The MMR process initiates when MutSα recognizes a mismatch on the daughter strand and recruits MutLα (48). To determine the role of hOrc6 in the MMR process, we addressed the association of MutSα and MutLα in cells lacking hOrc6. Using the PLA approach, we found that the interaction between members of the MutSα and MutLα was severely compromised (MSH6/MLH1 or MSH6/PMS2) in Orc6-depleted cells (Fig. 5*A*). However, the interaction between components of the MutSα complex itself (MSH2-MSH6) remained unaltered in cells lacking Orc6 (Fig. 5*B*). Next, we determined the status of the chromatin association of individual members of the MutSα and MutLα complexes in control and Orc6-depleted cells. DD-Orc6 cells were collected following the same protocol as shown in Fig. 3*D* to ensure cells were in S phase. Components of MutSα (MSH2 and MSH6) loaded onto the chromatin equally efficiently in control and Orc6-depleted cells (untreated as well as H_2O_2-treated cells; Fig. 5*C*). However, components of MutLα (MLH1 and PMS2) showed reduced chromatin association in H_2O_2-treated cells lacking Orc6

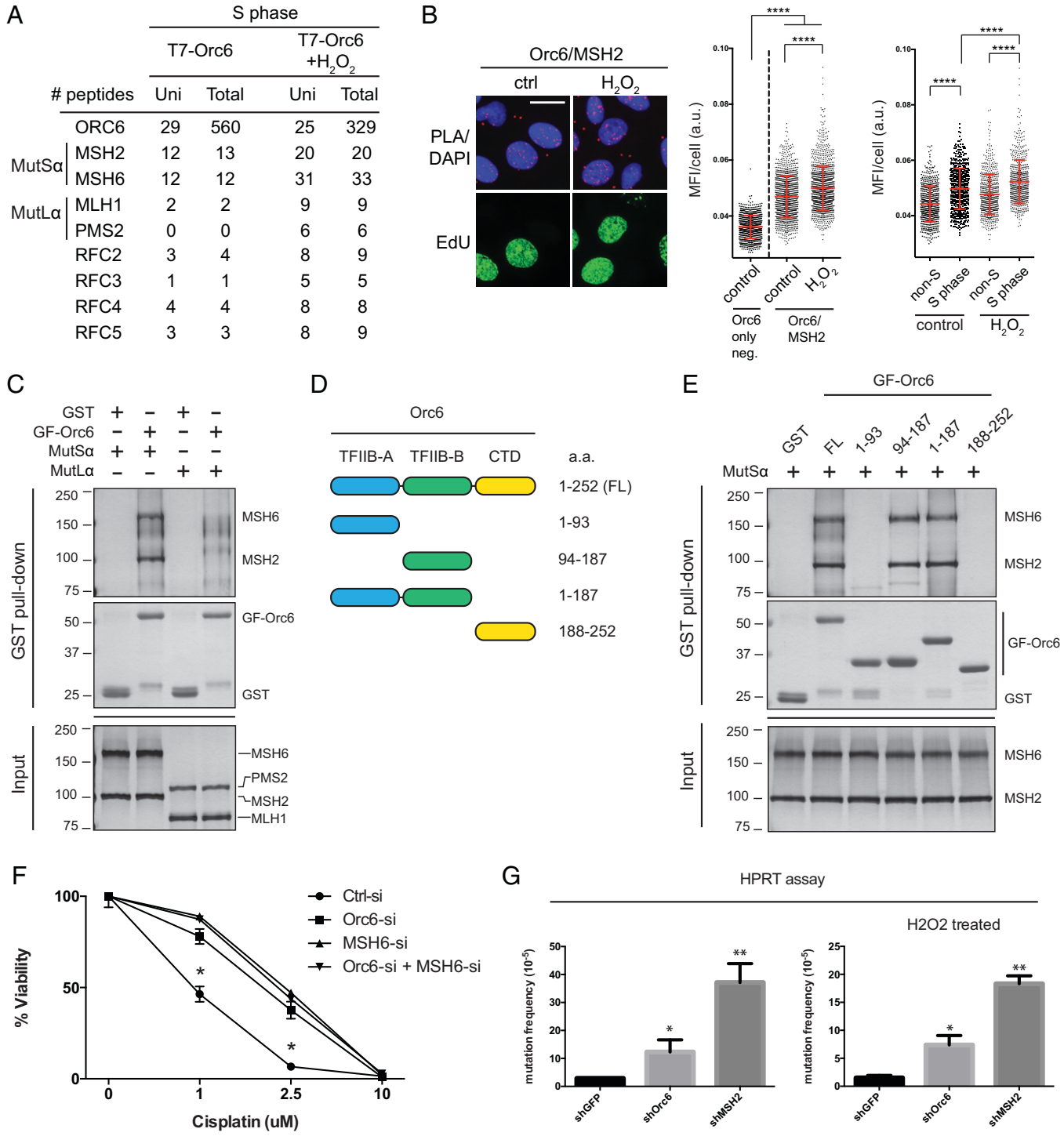

Fig. 4. Orc6 interacts with MutSα and functions in the MMR pathway. (*A*) MMR proteins identified by immunoprecipitation–mass spectrometry analysis from S-phase synchronized U2OS cells expressing T7-Orc6, with or without H_2O_2 treatment. For each protein, the numbers of unique peptides (Uni) and total peptides are presented. (*B*) Orc6 and MSH2 association by PLA (*Left*). EdU incorporation for determining S-phase cells. Scale bar, 25 μm. (*Middle*) Quantification of PLA. The first column represents a negative control (Ctrl) in which the MSH2 antibody was omitted. (*Right*) Further analysis of the quantification where S-phase (EdU-positive) and non–S-phase (EdU-negative) cells were separated in both control and H_2O_2 groups. Data are reported as mean ± SD. ****$P < 0.0001$ by unpaired two-tailed Student *t* test. (*C*) Direct interaction of Orc6 with MutSα or MutLα examined by GST pull-down assay. Proteins on sodium dodecyl–sulfate polyacrylamide gel electrophoresis gels were visualized by silver stain (*Upper* and the input image) or Coomassie stain (*Middle*). The background smears in GST-Flag-Orc6 (GF-Orc6; lanes 2 and 4) are nonspecific proteins from the preparation of GF-Orc6 beads. GST was a negative control. (*D*) Schematic illustration of Orc6 domains and different truncations. (*E*) Interaction of different truncations of GF-Orc6 with MutSα by GST pull-down assay. Proteins were visualized by silver stain (*Upper* and the input image) or Coomassie stain (*Middle*). (*F*) Clonogenic survival assay of cisplatin-treated control, Orc6, MSH6, or Orc6/MSH6 double knockdown U2OS cells. Data are reported as mean ± SD; $n = 3$. *$P < 0.05$ by unpaired two-tailed Student *t* test. (*G*) Mutation frequency determined by HPRT assay in A549 cells. Data are reported as mean ± SD; $n = 2$. *$P < 0.05$, **$P < 0.01$. a.u., arbitrary unit; a.a., amino acid; FL, full length; MFI, mean fluorescence intensity.

(Fig. 5*C*). These data demonstrate that hOrc6 is required for efficient MMR complex assembly on chromatin during oxidative DNA damage.

To further address the mechanism of how hOrc6 functions in MMR complex assembly, we tested if the Orc6 promotes the association between MutLα and MutSα. We performed an

in vitro coimmunoprecipitation assay to determine the level of MutLα recruitment to immobilized MutSα, using purified proteins in the presence or absence of DNA. We observed that in the presence of Orc6, MutLα binds more efficiently to MutSα (Fig. 5*D* and *SI Appendix*, Fig. S4*A*). It is known that the affinity between MutSα and MutLα strongly increases in the presence of mismatch-containing DNA, which we have observed in our coimmunoprecipitation. However, the enhanced affinity between MutSα and MutLα by Orc6 is mismatch independent, as we found the Orc6 facilitated the binding of MutLα to MutSα in all the experimental settings containing either heteroduplex DNA or homoduplex DNA (Fig. 5*D* and *SI Appendix*, Fig. S4*A*). Moreover, the TFIIB-B domain of Orc6 is sufficient to promote MutLα binding to MutSα (Fig. 5*E* and *SI Appendix*, Fig. S4*B*). Therefore, these data suggest that Orc6 is an accessory factor which, by binding to MutSα, increases the affinity of MutLα to MutSα.

Having established that hOrc6 plays a role in MMR complex assembly and that in the absence of hOrc6, MutLα is recruited inefficiently, we set out to address if hOrc6 promotes MMR activity. To this end, we performed the in vivo MMR assay, whereby we determined the reversion of a mutated codon within EGFP and quantified the activity by measuring EGFP signal in the cells (49). We prepared a heteroduplex plasmid containing a mispairing in the EGFP codon, where the sense strand is WT EGFP and the antisense strand has a mutation, which results in a premature stop codon (Fig. 5*F* and *SI Appendix*, Fig. S4*C*). Therefore, only when cells were able to repair the mismatch on the antisense strand could they express full-length WT EGFP and give a fluorescence signal. Using this assay, we quantified the extent of MMR activity in WT U2OS cells that were MMR proficient (35) and compared the activity to that in Orc6-depleted U2OS cells. We observed that depletion of hOrc6 caused significant reduction in EGFP signal intensity in the T/C heteroduplex (Fig. 5*G*), suggesting the important role of hOrc6 in supporting in vivo MMR. Moreover, double depletion of MSH6 and Orc6 did not further decrease the EGFP signal (Fig. 5 *H* and *I*). On the other hand, depletion of Orc2 did not show significant reduction of EGFP signal (*SI Appendix*, Fig. S4*D*). Future work will address the biochemical nature of Orc6 function in MMR. Our results collectively demonstrate that hOrc6 bound to MutSα facilitates the recruitment of MutLα to chromatin and that, in turn, is required for efficient MMR activity (Fig. 5*J*).

DISCUSSION

Primarily, based on studies from the yeast model system, Orc6, the smallest ORC subunit, is believed to function in DNA replication origin licensing and initiation. However, unlike other ORC subunits, function of human Orc6 is less clear due to its poorly conserved nature and conflicting biochemical data among species. In terms of replication licensing, recent structural studies have elucidated the requirement of yeast Orc6 in MCM loading (14, 43). However, it is still uncertain if human Orc6 functions the same way as in budding yeast. Our findings here suggest that hOrc6 is required during S phase, indicating divergent roles for Orc6 in human and yeast licensing processes. Recently, researchers using the CRISPR approach to knockout human Orc1, Orc2, Orc5, and Orc2/Orc5 reported that human core ORC is dispensable for replication (20, 50). Meanwhile, findings from another study continue to suggest the essentiality of ORC using ORC-specific CRISPR screens (51). In human cells, acute depletion of Orc1 and Orc2 resulted in defects in the chromatin loading of MCMs. Nevertheless, in our experimental system, Orc6 behaved differently in the sense that its depletion did not alter MCM loading to the chromatin. Our observations of an important S-phase phenotype in the same experimental system strongly argue the important function of Orc6 after origin licensing.

Yeast Orc6 is also required after the licensing steps, since depleting Orc6 after pre-RC formation has been shown to impair replication origin firing by destabilizing pre-RC (15). In human cells, we demonstrated that Orc6 associates with the replication fork and interacts with the components of the replication fork—observations that are also supported by proteomic data (40, 41). Using the DD-Orc6 to degrade Orc6 at specific stages of the cell cycle, we found that hOrc6 is essential for S-phase progression. Our results show that in human cells, Orc6 definitely functions after pre-RC formation.

MMR is a process that recognizes and fixes errors during DNA replication. Our results indicate that hOrc6 is an accessary factor of the MMR complex, promoting MMR complex assembly and activity (Fig. 5*H*). It is worth noting that although the structures of MutS and MutL are available, the interaction between them has been difficult to study (52). During the eukaryotic MMR process, MutSα recognizes the mismatch and undergoes ATP-dependent conformational changes that allow the binding of MutLα. This MutSα–MutLα complex is very transient and dynamic. By using site-specific crosslinking, the transient *Escherichia coli* MutS–MutL complex was successfully captured, providing valuable information about the MutS conformation when interacting with MutL (53). However, the information about the human MutSα–MutLα structure is still lacking. It is also unclear if, in vivo, there is any additional factor influencing the MMR complex assembly. Our results indicating that the association of Orc6 with MutSα increases the affinity of MutLα binding to MutSα are, therefore, of great importance for the MMR field. It is worth noting, however, that the TFIIB-B domain of hOrc6, which is required for MMR function, as we demonstrated in this work, is also the main region that mediates its DNA binding (18). This makes it difficult to functionally separate hOrc6's role in MMR and S-phase progression. Further investigation is required to address this question. We propose that the binding of Orc6, as an accessory factor, stabilizes the MutSα at a conformation that allows MutLα to bind and function. Structural studies are also needed to investigate how hOrc6 influences MutSα structure.

During MMR, ssDNA is an important intermediate generated by EXO1 excision after the incision step (29, 54–56). More recently, it has been shown that MMR processing of a methylation-induced DNA lesion behind the replication fork causes ssDNA accumulation, interrupts fork progression, and might induce replication stress (57). Thus, inefficient MMR activity could lead to reduced ssDNA generation. This is consistent with the defects in ssDNA generation that we observed in hOrc6-depleted cells. This finding is further corroborated by the fact that cells treated with oxidative or alkylating agents had increased DNA damage without Orc6. Since there is not an efficient way to specifically induce mismatch on DNA, most studies utilize oxidative or alkylating agents. Base excision repair and nucleotide excision repair are believed to be the two main pathways that remove these lesions. However, studies suggest that MMR is also critical for the response to oxidative DNA damage (58). Moreover, defects in MMR activity directly lead to reduced ATR signaling, as knockdown of MSH2 causes reduced Chk1 phosphorylation (59). Additionally, recognition of O6-meG/T mispairings by MutSα and MutLα directly

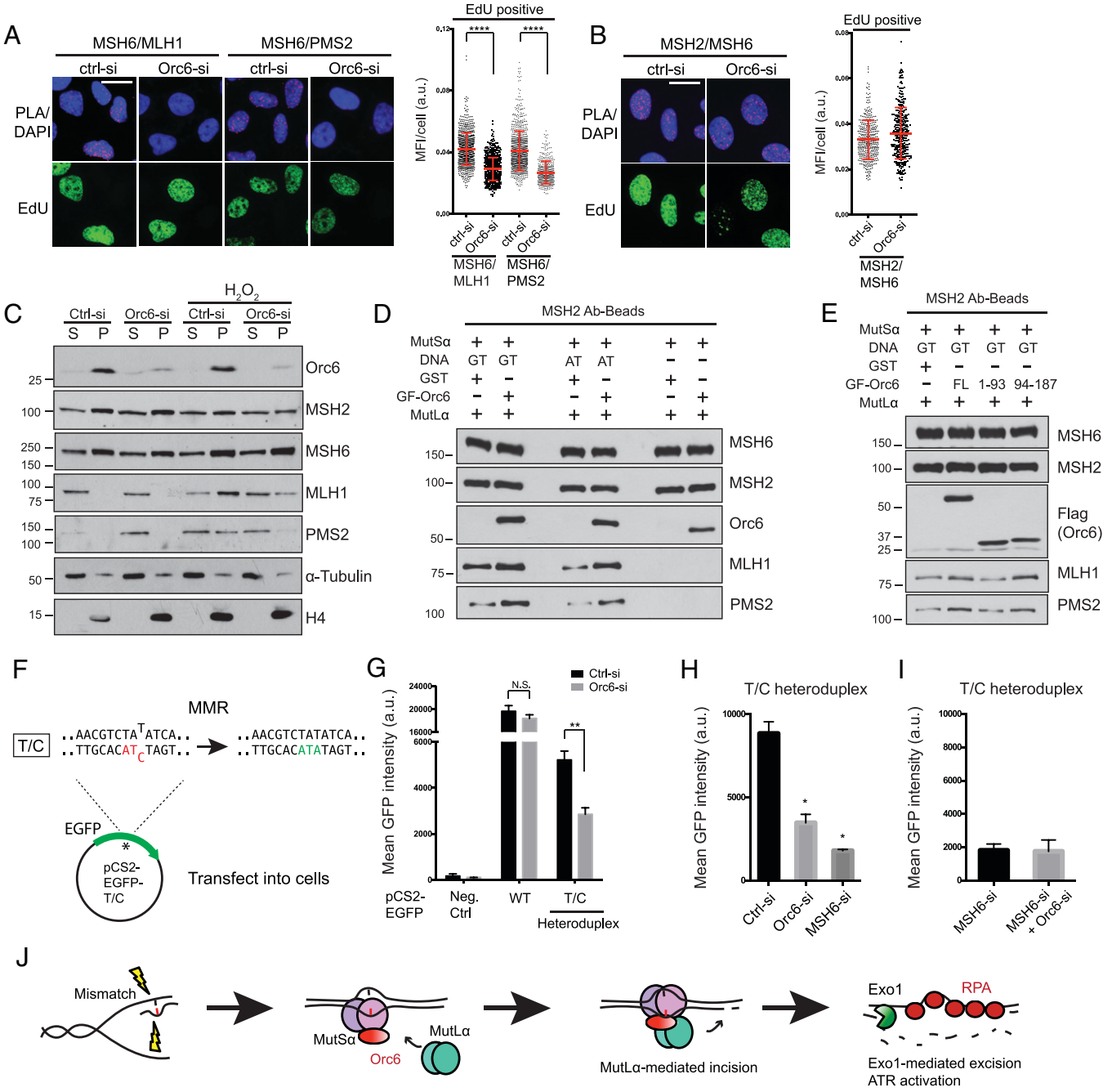

Fig. 5. Orc6 facilitates MutLα recruitment to MutSα. (*A*) Interaction between MSH6/MLH1 and MSH6/PMS2 quantified by PLA in control and Orc6-depleted U2OS cells. Representative images (*Left*) and quantification of the interaction in S-phase cells (*Right*) are shown. Scale bar, 25 μm. Data are reported as mean ± SD. ****$P < 0.0001$ by unpaired two-tailed Student *t* test. (*B*) Formation of MSH2/MSH6 complex (MutSα heterodimer) examined by PLA; representative images (*Left*) and quantification (*Right*) are shown. Scale bar, 25 μm. Data are reported as mean ± SD. (*C*) Western blot analysis of chromatin fractionation samples. The samples were prepared following the same protocol as in *D*. (*D*) Effect of Orc6 on the in vitro recruitment of MutLα to MutSα in no DNA, homoduplex DNA, or G/T mismatch DNA. GST as a control (Ctrl). *SI Appendix*, Fig. S4*A* shows quantification. (*E*) In vitro recruitment of MutLα to MutSα using Orc6 full-length (FL) or different TFIIB-B domains. *SI Appendix*, Fig. S4*B* shows quantification. (*F*) Illustration of the heteroduplex repair during the MMR assay. (*G*) Quantification of MMR activity of Orc6-depleted U2OS cells. Mean GFP intensity was measured using flow cytometry. Data are reported as mean ± SD; $n = 3$. *$P < 0.05$, **$P < 0.01$ by unpaired two-tailed Student *t* test. (*H*) Quantification of MMR activity of Orc6 knockdown compared with MSH6 knockdown. Data are reported as mean ± SD; $n = 2$. *$P < 0.05$ by unpaired two-tailed Student *t* test. (*I*) MMR activity of MSH6 and Orc6 double knockdown. Data are reported as mean ± SD; $n = 5$. (*J*) Model for Orc6 function in facilitating the assembly of MMR complex for efficient repair and ATR activation. Ab, antibody; a.u., arbitrary unit; GF-Orc6, GST-Flag-Orc6; MFI, mean fluorescence intensity; N.S., not significant; S, soluble; P, chromatin fraction.

recruits and activates the ATR/ATRIP complex independent of RPA–ssDNA (60). Thus, our finding that ATR is not fully activated in hOrc6-depleted cells is likely due to a defective MMR pathway. Moreover, prior proteomic study has pointed to connections between the DNA damage response (including the MSH module and ATR/FANC module) and DNA replication (including the ORC module and RFC module) components suggesting that many repair pathways are part of a larger network dedicated to DNA replication. Furthermore, MSH components and ORC subunits were found to be substrates and potentially regulated by the ATM/ATR signaling network (61). The connections between DNA repair and DNA replication are highly complex and remain an area of intense research. Together, our results point to a regulatory mechanism in human cells

whereby Orc6 travels along with replisome and acts as an accessory factor of MutSα upon encountering a mismatch, and promotes MMR complex formation to facilitate DNA damage repair and ATR activation.

It is well known that defects in MMR cause errors during DNA replication and are linked to a hereditary cancer syndrome, Lynch syndrome, often associated with microsatellite instability (62). Furthermore, colorectal tumors are often associated with defects in MMR (63). It is worth noting that Orc6 levels are highly elevated in colorectal cancers (64), and the reduction of Orc6 sensitizes colorectal cancer cells to chemotherapeutic drugs (65). Moreover, *ORC6* has been included as a predictor in three commonly used, prognostic, multigene expression profiles for breast cancer (66). It has been known for a long time that the misregulation of Orc6 correlates with genome instability, yet the molecular details had remained to be elucidated. Our present studies provide insights into the role of Orc6 in the maintenance of genome integrity.

Materials and Methods

A detailed description of all the cell lines, plasmids, antibodies, and experimental procedures can be found in the *SI Materials and Methods*. Experimental procedures included iPOND assay, SIRF, PLA, comet assay, DNA fiber analysis, clonogenic survival assay, GST–pull-down assay, MMR in vivo assay, HPRT assay, and the single-molecule pull-down assay. Details of quantifications and statistical analyses are also included.

Data Availability. All study data are included in the article and/or supporting information.

ACKNOWLEDGMENTS. We thank members of the S.G.P. and K.V.P. laboratory for discussions and suggestions. We thank Drs. M. Aladjem, J. Cook, A. Dutta, M. Mechali, B. Moriarity, S. Nair, B. Stillman, M. Wold, and L. Zou for providing reagents and suggestions. We thank Dr. D. Rivier for critical reading of the manuscript. This work was supported by an NSF–Cellular and Molecular Mechanics and BioNanotechnology–Integrative Graduate Education and Research Traineeship fellowship to R.Y.C.H.; NIH (R35 GM 122569) and NSF (PHY 1430124) awards to T.H.; NIH award (R01GM132128) to F.A.K.; Cancer Center at Illinois seed grant and Prairie Dragon Paddlers and NSF Early-Concept Grants for Exploratory Research (grant MCB1723008) awards and NIH grant R01GM132458 and R21AG065748 to K.V.P.; and Cancer Center at Illinois seed grant, NSF (1243372 and 1818286) and NIH (R01GM125196) awards to S.G.P. T.H. is an investigator with Howard Hughes Medical Institute.

Author affiliations: [a]Department of Cell and Developmental Biology, University of Illinois at Urbana–Champaign, Urbana, IL 61801; [b]Department of Biochemistry and Molecular Biology, Southern Illinois University School of Medicine, Carbondale, IL 62901; [c]Biophysics and Biophysical Chemistry, Johns Hopkins University, Baltimore, MD 21205; [d]HHMI, Johns Hopkins University, Baltimore, MD 21205; and [e]Cancer Center at Illinois, University of Illinois at Urbana–Champaign, Urbana, IL 61801

1. S. P. Bell, B. Stillman, ATP-dependent recognition of eukaryotic origins of DNA replication by a multiprotein complex. *Nature* **357**, 128–134 (1992).
2. I. N. Chesnokov, Multiple functions of the origin recognition complex. *Int. Rev. Cytol.* **256**, 69–109 (2007).
3. T. Sasaki, D. M. Gilbert, The many faces of the origin recognition complex. *Curr. Opin. Cell Biol.* **19**, 337–343 (2007).
4. L. S. Bicknell *et al.*, Mutations in the pre-replication complex cause Meier-Gorlin syndrome. *Nat. Genet.* **43**, 356–359 (2011).
5. M. Hossain, B. Stillman, Meier-Gorlin syndrome mutations disrupt an Orc1 CDK inhibitory domain and cause centrosome reduplication. *Genes Dev.* **26**, 1797–1810 (2012).
6. F. Bleichert *et al.*, A Meier-Gorlin syndrome mutation in a conserved C-terminal helix of Orc6 impedes origin recognition complex formation. *eLife* **2**, e00882 (2013).
7. S. P. Bell, A. Dutta, DNA replication in eukaryotic cells. *Annu. Rev. Biochem.* **71**, 333–374 (2002).
8. S. K. Dhar, A. Dutta, Identification and characterization of the human ORC6 homolog. *J. Biol. Chem.* **275**, 34983–34988 (2000).
9. K. Siddiqui, B. Stillman, ATP-dependent assembly of the human origin recognition complex. *J. Biol. Chem.* **282**, 32370–32383 (2007).
10. S. Vashee, P. Simancek, M. D. Challberg, T. J. Kelly, Assembly of the human origin recognition complex. *J. Biol. Chem.* **276**, 26666–26673 (2001).
11. I. Chesnokov, D. Remus, M. Botchan, Functional analysis of mutant and wild-type *Drosophila* origin recognition complex. *Proc. Natl. Acad. Sci. U.S.A.* **98**, 11997–12002 (2001).
12. P. J. Gillespie, A. Li, J. J. Blow, Reconstitution of licensed replication origins on *Xenopus* sperm nuclei using purified proteins. *BMC Biochem.* **2**, 15 (2001).
13. S. K. Dhar, L. Delmolino, A. Dutta, Architecture of the human origin recognition complex. *J. Biol. Chem.* **276**, 29067–29071 (2001).
14. N. Li *et al.*, Structure of the origin recognition complex bound to DNA replication origin. *Nature* **559**, 217–222 (2018).
15. J. W. Semple *et al.*, An essential role for Orc6 in DNA replication through maintenance of pre-replicative complexes. *EMBO J.* **25**, 5150–5158 (2006).
16. S. Chen, M. A. de Vries, S. P. Bell, Orc6 is required for dynamic recruitment of Cdt1 during repeated Mcm2-7 loading. *Genes Dev.* **21**, 2897–2907 (2007).
17. M. Balasov, R. P. Huijbregts, I. Chesnokov, Role of the Orc6 protein in origin recognition complex-dependent DNA binding and replication in *Drosophila melanogaster*. *Mol. Cell. Biol.* **27**, 3143–3153 (2007).
18. N. Xu *et al.*, Structural basis of DNA replication origin recognition by human Orc6 protein binding with DNA. *Nucleic Acids Res.* **48**, 11146–11161 (2020).
19. A. W. Thomae *et al.*, Different roles of the human Orc6 protein in the replication initiation process. *Cell. Mol. Life Sci.* **68**, 3741–3756 (2011).
20. E. Shibata, A. Dutta, A human cancer cell line initiates DNA replication normally in the absence of ORC5 and ORC2 proteins. *J. Biol. Chem.* **295**, 16949–16959 (2020).
21. I. N. Chesnokov, O. N. Chesnokova, M. Botchan, A cytokinetic function of *Drosophila* ORC6 protein resides in a domain distinct from its replication activity. *Proc. Natl. Acad. Sci. U.S.A.* **100**, 9150–9155 (2003).
22. S. G. Prasanth, K. V. Prasanth, B. Stillman, Orc6 involved in DNA replication, chromosome segregation, and cytokinesis. *Science* **297**, 1026–1031 (2002).
23. D. Cortez, Replication-coupled DNA repair. *Mol. Cell* **74**, 866–876 (2019).
24. T. A. Kunkel, D. A. Erie, Eukaryotic mismatch repair in relation to DNA replication. *Annu. Rev. Genet.* **49**, 291–313 (2015).
25. H. Flores-Rozas, D. Clark, R. D. Kolodner, Proliferating cell nuclear antigen and Msh2p-Msh6p interact to form an active mispair recognition complex. *Nat. Genet.* **26**, 375–378 (2000).
26. L. Gu, Y. Hong, S. McCulloch, H. Watanabe, G. M. Li, ATP-dependent interaction of human mismatch repair proteins and dual role of PCNA in mismatch repair. *Nucleic Acids Res.* **26**, 1173–1178 (1998).
27. H. Hombauer, A. Srivatsan, C. D. Putnam, R. D. Kolodner, Mismatch repair, but not heteroduplex rejection, is temporally coupled to DNA replication. *Science* **334**, 1713–1716 (2011).
28. H. E. Kleczkowska, G. Marra, T. Lettieri, J. Jiricny, hMSH3 and hMSH6 interact with PCNA and colocalize with it to replication foci. *Genes Dev.* **15**, 724–736 (2001).
29. F. A. Kadyrov, L. Dzantiev, N. Constantin, P. Modrich, Endonucleolytic function of MutLα in human mismatch repair. *Cell* **126**, 297–308 (2006).
30. T. T. Schmidt, H. Hombauer, Visualization of mismatch repair complexes using fluorescence microscopy. *DNA Repair (Amst.)* **38**, 58–67 (2016).
31. A. G. Schroering, M. A. Edelbrock, T. J. Richards, K. J. Williams, The cell cycle and DNA mismatch repair. *Exp. Cell Res.* **313**, 292–304 (2007).
32. M. A. Edelbrock, S. Kaliyaperumal, K. J. Williams, DNA mismatch repair efficiency and fidelity are elevated during DNA synthesis in human cells. *Mutat. Res.* **662**, 59–66 (2009).
33. S. W. Awwad, N. Ayoub, Overexpression of KDM4 lysine demethylases disrupts the integrity of the DNA mismatch repair pathway. *Biol. Open* **4**, 498–504 (2015).
34. J. E. Loughery *et al.*, DNMT1 deficiency triggers mismatch repair defects in human cells through depletion of repair protein levels in a process involving the DNA damage response. *Hum. Mol. Genet.* **20**, 3241–3255 (2011).
35. B. Schöpf *et al.*, Interplay between mismatch repair and chromatin assembly. *Proc. Natl. Acad. Sci. U.S.A.* **109**, 1895–1900 (2012).
36. F. Yuan, L. Gu, S. Guo, C. Wang, G. M. Li, Evidence for involvement of HMGB1 protein in human DNA mismatch repair. *J. Biol. Chem.* **279**, 20935–20940 (2004).
37. L. Y. Kadyrova, E. R. Blanko, F. A. Kadyrov, CAF-I-dependent control of degradation of the discontinuous strands during mismatch repair. *Proc. Natl. Acad. Sci. U.S.A.* **108**, 2753–2758 (2011).
38. F. Li *et al.*, The histone mark H3K36me3 regulates human DNA mismatch repair through its interaction with MutSα. *Cell* **153**, 590–600 (2013).
39. S. Roy, J. W. Luzwick, K. Schlacher, SIRF: Quantitative in situ analysis of protein interactions at DNA replication forks. *J. Cell Biol.* **217**, 1521–1536 (2018).
40. C. Alabert *et al.*, Nascent chromatin capture proteomics determines chromatin dynamics during DNA replication and identifies unknown fork components. *Nat. Cell Biol.* **16**, 281–293 (2014).
41. S. R. Wessel, K. N. Mohni, J. W. Luzwick, H. Dungrawala, D. Cortez, Functional analysis of the replication fork proteome identifies BET proteins as PCNA regulators. *Cell Rep.* **28**, 3497–3509.e4 (2019).
42. S. Giri *et al.*, The preRC protein ORCA organizes heterochromatin by assembling histone H3 lysine 9 methyltransferases on chromatin. *eLife* **4**, e06496 (2015).
43. T. C. R. Miller, J. Locke, J. F. Greiwe, J. F. X. Diffley, A. Costa, Mechanism of head-to-head MCM double-hexamer formation revealed by cryo-EM. *Nature* **575**, 704–710 (2019).
44. J. P. Matson *et al.*, Rapid DNA replication origin licensing protects stem cell pluripotency. *eLife* **6**, e30473 (2017).
45. S. Yan, M. Sorrell, Z. Berman, Functional interplay between ATM/ATR-mediated DNA damage response and DNA repair pathways in oxidative stress. *Cell. Mol. Life Sci.* **71**, 3951–3967 (2014).
46. J. T. Drummond, A. Anthoney, R. Brown, P. Modrich, Cisplatin and adriamycin resistance are associated with MutLα and mismatch repair deficiency in an ovarian tumor cell line. *J. Biol. Chem.* **271**, 19645–19648 (1996).
47. J. Wu, L. Gu, H. Wang, N. E. Geacintov, G. M. Li, Mismatch repair processing of carcinogen-DNA adducts triggers apoptosis. *Mol. Cell. Biol.* **19**, 8292–8301 (1999).
48. G. X. Reyes, T. T. Schmidt, R. D. Kolodner, H. Hombauer, New insights into the mechanism of DNA mismatch repair. *Chromosoma* **124**, 443–462 (2015).

49. S. Traver *et al.*, MCM9 is required for mammalian DNA mismatch repair. *Mol. Cell* **59**, 831–839 (2015).
50. E. Shibata *et al.*, Two subunits of human ORC are dispensable for DNA replication and proliferation. *eLife* **5**, e19084 (2016).
51. H. C. Chou *et al.*, The human origin recognition complex is essential for pre-RC assembly, mitosis, and maintenance of nuclear structure. *eLife* **10**, e61797 (2021).
52. P. Friedhoff, P. Li, J. Gotthardt, Protein-protein interactions in DNA mismatch repair. *DNA Repair (Amst.)* **38**, 50–57 (2016).
53. F. S. Groothuizen *et al.*, MutS/MutL crystal structure reveals that the MutS sliding clamp loads MutL onto DNA. *eLife* **4**, e06744 (2015).
54. Y. Zhang *et al.*, Reconstitution of 5′-directed human mismatch repair in a purified system. *Cell* **122**, 693–705 (2005).
55. J. Genschel, P. Modrich, Mechanism of 5′-directed excision in human mismatch repair. *Mol. Cell* **12**, 1077–1086 (2003).
56. N. Constantin, L. Dzantiev, F. A. Kadyrov, P. Modrich, Human mismatch repair: Reconstitution of a nick-directed bidirectional reaction. *J. Biol. Chem.* **280**, 39752–39761 (2005).
57. D. Gupta, B. Lin, A. Cowan, C. D. Heinen, ATR-Chk1 activation mitigates replication stress caused by mismatch repair-dependent processing of DNA damage. *Proc. Natl. Acad. Sci. U.S.A.* **115**, 1523–1528 (2018).
58. G. Bridge, S. Rashid, S. A. Martin, DNA mismatch repair and oxidative DNA damage: Implications for cancer biology and treatment. *Cancers (Basel)* **6**, 1597–1614 (2014).
59. Y. Wang, J. Qin, MSH2 and ATR form a signaling module and regulate two branches of the damage response to DNA methylation. *Proc. Natl. Acad. Sci. U.S.A.* **100**, 15387–15392 (2003).
60. K. Yoshioka, Y. Yoshioka, P. Hsieh, ATR kinase activation mediated by MutSα and MutLalpha in response to cytotoxic O6-methylguanine adducts. *Mol. Cell* **22**, 501–510 (2006).
61. S. Matsuoka *et al.*, ATM and ATR substrate analysis reveals extensive protein networks responsive to DNA damage. *Science* **316**, 1160–1166 (2007).
62. E. M. Goellner, Chromatin remodeling and mismatch repair: Access and excision. *DNA Repair (Amst.)* **85**, 102733 (2020).
63. S. K. H. Li, A. Martin, Mismatch repair and colon cancer: Mechanisms and therapies explored. *Trends Mol. Med.* **22**, 274–289 (2016).
64. Y. Xi, A. Formentini, G. Nakajima, M. Kornmann, J. Ju, Validation of biomarkers associated with 5-fluorouracil and thymidylate synthase in colorectal cancer. *Oncol. Rep.* **19**, 257–262 (2008).
65. E. J. Gavin, B. Song, Y. Wang, Y. Xi, J. Ju, Reduction of Orc6 expression sensitizes human colon cancer cells to 5-fluorouracil and cisplatin. *PLoS One* **3**, e4054 (2008).
66. T. A. Koleck, Y. P. Conley, Identification and prioritization of candidate genes for symptom variability in breast cancer survivors based on disease characteristics at the cellular level. *Breast Cancer (Dove Med. Press)* **8**, 29–37 (2016).